

# Inhibition of Endoplasmic Reticulum-Resident Glucosidases Impairs Severe Acute Respiratory Syndrome Coronavirus and Human Coronavirus NL63 Spike Protein-Mediated Entry by Altering the Glycan Processing of Angiotensin I-Converting Enzyme 2

Xuesen Zhao,<sup>a,b</sup> Fang Guo,<sup>a</sup> Mary Ann Comunale,<sup>a</sup> Anand Mehta,<sup>a</sup> Mohit Sehgal,<sup>a</sup> Pooja Jain,<sup>a</sup> Andrea Cuconati,<sup>b</sup> Hanxin Lin,<sup>c</sup> Timothy M. Block,<sup>a,b</sup> Jinhong Chang,<sup>a</sup> Ju-Tao Guo<sup>a</sup>

Drexel Institute for Biotechnology and Virology Research, Department of Microbiology and Immunology, Drexel University College of Medicine, Doylestown, Pennsylvania, USA<sup>a</sup>; Baruch S. Blumberg Institute, Hepatitis B Foundation, Doylestown, Pennsylvania, USA<sup>b</sup>; Department of Pathology and Molecular Medicine, McMaster University, Hamilton, Canada<sup>c</sup>

**Endoplasmic reticulum (ER)-resident glucosidases I and II sequentially trim the three terminal glucose moieties on the N-linked glycans attached to nascent glycoproteins. These reactions are the first steps of N-linked glycan processing and are essential for proper folding and function of many glycoproteins. Because most of the viral envelope glycoproteins contain N-linked glycans, inhibition of ER glucosidases with derivatives of 1-deoxynojirimycin, i.e., iminosugars, efficiently disrupts the morphogenesis of a broad spectrum of enveloped viruses. However, like viral envelope proteins, the cellular receptors of many viruses are also glycoproteins. It is therefore possible that inhibition of ER glucosidases not only compromises virion production but also disrupts expression and function of viral receptors and thus inhibits virus entry into host cells. Indeed, we demonstrate here that iminosugar treatment altered the N-linked glycan structure of angiotensin I-converting enzyme 2 (ACE2), which did not affect its expression on the cell surface or its binding of the severe acute respiratory syndrome coronavirus (SARS-CoV) spike glycoprotein. However, alteration of N-linked glycans of ACE2 impaired its ability to support the transduction of SARS-CoV and human coronavirus NL63 (HCoV-NL63) spike glycoprotein-pseudotyped lentiviral particles by disruption of the viral envelope protein-triggered membrane fusion. Hence, in addition to reducing the production of infectious virions, inhibition of ER glucosidases also impairs the entry of selected viruses via a post-receptor-binding mechanism.**

Development of antiviral agents targeting virus-encoded enzymes has achieved great success in the last few decades. However, the antiviral activity of these direct-acting antiviral agents is usually virus specific, and treatment failure occurs due to the emergence of drug-resistant viruses. To overcome these problems, it has been speculated that targeting host functions essential for viral replication should have a much higher genetic barrier for drug resistance and may inhibit all the viruses that depend on the targeted host function (1, 2). Host-targeting broad-spectrum antiviral agents are particularly attractive for treatment of viral hemorrhagic fever and respiratory tract viral infections. This is because each of these medical conditions can be caused by many viruses from different families, for which development of virus-specific antiviral agents would be a daunting task. Although many host cellular functions have been demonstrated to be essential for viral replication in cultured cells (3–6), only a few cellular enzymes, including IMP dehydrogenase (IMPDH) (7), S-adenosyl-L-homocysteine (SAH) hydrolase (8, 9), cyclophilin (10), and endoplasmic reticulum (ER) glucosidases (11), have thus far been validated *in vivo* as host targets for broad-spectrum antiviral agents.

ER glucosidases I and II sequentially trim the three terminal glucose moieties on the N-linked glycans attached to nascent glycoproteins. These reactions are the first steps of N-linked glycan processing and are essential for proper folding and function of many glycoproteins. Because most viral envelope glycoproteins contain N-linked glycans, ER glucosidase inhibitors, particularly 1-deoxynojirimycin (DNJ) and castanospermine (CAST) derivatives, i.e., iminosugars, have been investigated in the last 3 decades

as broad-spectrum antiviral agents (11). Indeed, overwhelming evidence suggests that iminosugars disrupt the glycan processing of viral envelope proteins, which results in their misfolding and degradation and, consequently, in a reduction of infectious virion production (12, 13). Moreover, antiviral activities of several iminosugar compounds against dengue virus (DENV) (14–19), Japanese encephalitis virus (JEV) (20), Ebola virus (EBOV), and Marburg virus (21) have been demonstrated in mice. 6-O-Butanoyl-CAST was shown in a human clinical trial to reduce the load of hepatitis C virus (HCV) in peripheral blood (22).

While prior studies clearly indicate that inhibition of ER glucosidases is an efficacious and well-tolerated therapeutic approach against a broad spectrum of enveloped viruses (22, 23), it is im-

Received 30 July 2014 Returned for modification 20 August 2014

Accepted 15 October 2014

Accepted manuscript posted online 27 October 2014

Citation Zhao X, Guo F, Comunale MA, Mehta A, Sehgal M, Jain P, Cuconati A, Lin H, Block TM, Chang J, Guo J-T. 2015. Inhibition of endoplasmic reticulum-resident glucosidases impairs severe acute respiratory syndrome coronavirus and human coronavirus NL63 spike protein-mediated entry by altering the glycan processing of angiotensin I-converting enzyme 2. *Antimicrob Agents Chemother* 59:206–216. doi:10.1128/AAC.03999-14.

Address correspondence to Ju-Tao Guo, Ju-Tao.Guo@drexelmed.edu.

X.Z. and F.G. contributed equally to this article.

Copyright © 2015, American Society for Microbiology. All Rights Reserved.

doi:10.1128/AAC.03999-14

portant to determine whether suppression of the host cellular N-linked glycan processing enzymes affects cellular glycoprotein metabolism and function, particularly those required for virus infections. For instance, like viral envelope proteins, the cellular receptors of many viruses are also glycoproteins. It is therefore conceivable that inhibition of ER  $\alpha$ -glucosidases may not only suppress virion production but also disrupt expression and function of viral receptors and thus inhibit virus entry into host cells.

In our efforts to investigate this hypothesis, we found and report herein that iminosugar treatment did not apparently inhibit the transduction of lentiviral particles pseudotyped with envelope proteins derived from HCV, vesicular stomatitis virus (VSV), Moloney murine leukemia virus (MLV), EBOV, and Lassa fever virus (LASV). However, the transduction of lentiviral particles pseudotyped with envelope glycoproteins derived from severe acute respiratory syndrome coronavirus (SARS-CoV), human coronavirus NL63 (HCoV-NL63), and influenza A virus (IAV) was significantly inhibited by iminosugars. Further mechanistic studies revealed that iminosugar treatment altered the glycan structure of angiotensin I-converting enzyme 2 (ACE2), the cellular receptor of SARS-CoV and HCoV-NL63 (24, 25). Alteration of N-linked glycans of ACE2 does not apparently affect its cell surface expression or binding to SARS-CoV spike glycoprotein, but it does impair the viral envelope spike glycoprotein-triggered membrane fusion. Hence, our work supports the hypothesis that in addition to disrupting the morphogenesis of a broad spectrum of enveloped viruses, suppression of ER glucosidases also impairs the entry of certain human viruses by altering the glycan structures of their cellular receptors.

## MATERIALS AND METHODS

**Cell cultures.** The human hepatoma cell line Huh7.5 was cultured in Dulbecco's modified Eagle's medium (DMEM) supplemented with 10% fetal bovine serum (FBS), penicillin G, streptomycin, nonessential amino acids, and 2 mM L-glutamine. FLP-IN T Rex 293 cells were purchased from Invitrogen and maintained in DMEM supplemented with 10% FBS, penicillin G, streptomycin, 10  $\mu$ g/ml blasticidin, and 100  $\mu$ g/ml Zeocin (26).

**Chemicals and antibodies.** Iminosugar compounds *N*-butyl-DNJ (NB-DNJ), CM-10-18, IHVR-11029, and IHVR-17028 were synthesized as previously described (27, 28). A polyclonal antibody against human ACE2 was purchased from R&D Systems, and a  $\beta$ -actin monoclonal antibody was purchased from Sigma. A mouse monoclonal antibody against the myc epitope was obtained from Pierce.

**Plasmids.** Plasmids expressing VSV G protein, Lassa fever virus glycoprotein (GP), Ebola virus envelope glycoprotein, SARS-CoV spike glycoprotein, NL63 spike glycoprotein, H1N1 influenza A virus (A/WSN/33) hemagglutinin (HA) and neuraminidase (NA), and HCV E1 and E2 proteins were described previously (21, 29, 30). A plasmid expressing the MLV envelope protein was purchased from Clontech. Plasmid pNL4.3.Luc.R<sup>-</sup>E<sup>-</sup> was obtained through the NIH AIDS Research and Reference Reagent Program (31, 32). An ACE2 cDNA clone was obtained from Origene. A myc tag was added to the N terminus of ACE2 by PCR and cloned into the pcDNA5/FRT/ $\Delta$ CAT vector (Invitrogen) to yield plasmid pcDNA5/RFT/ACE2. A plasmid encoding a fusion protein of the receptor binding domain (RBD) of SARS-CoV spike glycoprotein (amino acids [aa] 318 to 510) and the human immunoglobulin (Ig) Fc fragment was described previously (33). Plasmids pT7/Luc and pCMV/T7 pol were purchased from Clontech.

**Establishment of 293-derived cell lines expressing human ACE2 in a Tet-inducible manner.** As previously described (26, 34), FLP-IN T Rex 293 cells were cotransfected with pOG44 and pcDNA5/RFT/ACE2 at a molar ratio of 1:1. Two days after transfection, cells were trypsinized and

reseeded at less than 25% confluence. The cDNA-integrated cells were selected with 250  $\mu$ g/ml hygromycin and 5  $\mu$ g/ml blasticidin. Two weeks later, separate colonies appeared, and the pool of such cells was expanded to generate a cell line, designated FLP-IN/ACE2, that expresses ACE2 proteins upon the addition of tetracycline (Tet) to the culture medium. To ensure tight control of target gene expression by tetracycline, the cell line was selected and maintained in DMEM supplemented with 10% certified tetracycline-free FBS (HyClone). Expression of human ACE2 by the cell line was confirmed by Western blotting with an antibody against the myc tag.

**Packaging of pseudotyped retroviral particles.** The pseudotyped lentiviral particles were packaged in Lenti-X 293T cells. Briefly,  $2 \times 10^6$  Lenti-X 293T cells were seeded into a 100-mm-diameter dish 1 day prior to transfection. Cells were cotransfected with 20  $\mu$ g of pNL4.3.Luc.R<sup>-</sup>E<sup>-</sup> and 10  $\mu$ g of plasmid expressing a virus envelope protein by using the calcium phosphate precipitation procedure. At 24 h posttransfection, the cells were replenished with complete DMEM. The culture supernatants were harvested 48 h after the transfection, filtered through a 0.45- $\mu$ m-pore-size PES syringe filter (Millipore), aliquoted, and stored at  $-80^\circ\text{C}$  until use.

**Pseudotyped lentiviral particle transduction and luciferase assay.** Huh7.5 or FLP-IN/ACE2 cells seeded in 96-well plates with black walls and clear bottoms were pretreated with 50  $\mu$ M iminosugar IHVR-17028 for the indicated period or during infection of pseudotyped lentiviral particles for 2 h. In our studies, each pseudotype was titrated by infection of cells with different amounts of pseudotype preparations. The inhibition by iminosugars of the transduction of a given pseudotype was determined by the amounts of pseudotype particles that yielded luciferase signals of 10,000 to 1,000,000 light units per well. The infected cells were replenished with fresh medium. At 2 days postinfection, the medium was removed and cells were lysed with 20  $\mu$ l/well of cell lysis buffer (Promega) for 15 min, followed by adding 50  $\mu$ l/well of luciferase substrate (Promega). The firefly luciferase activities were measured by luminometry in a TopCounter instrument (PerkinElmer).

**Western blot assay.** Cell monolayers were washed once with phosphate-buffered saline (PBS) and lysed with  $1 \times$  Laemmli buffer. An aliquot of cell lysate was separated in NuPAGE Novex 4 to 12% Bis-Tris gel (Invitrogen) and electrophoretically transferred to a nitrocellulose membrane (Invitrogen). The membranes were blocked with phosphate-buffered saline containing 5% nonfat dry milk and probed with the desired antibody. The bound antibodies were visualized by use of IRDye secondary antibodies and imaging with a Li-Cor Odyssey system (Li-Cor Biotechnology).

**Glycan analysis.** FLP-IN/ACE2 cells were cultured with complete DMEM containing 1  $\mu$ g/ml tetracycline to induce ACE2 expression and then mock treated or treated with 50  $\mu$ M IHVR-17028 for 48 h. The cells were then lysed with 3-[(3-cholamidopropyl)-dimethylammonio]-1-propanesulfonate (CHAPS) buffer (10 mM Tris-HCl, pH 7.5, 150 mM NaCl, and 1% CHAPS). ACE2 protein was immunoprecipitated with a monoclonal antibody against the myc epitope, followed by incubation with protein A/G-agarose beads (Pierce) and washing with CHAPS buffer. The immunocomplexes were denatured with Laemmli SDS protein loading buffer, resolved in a 10% Tris-glycine gel (Invitrogen), and stained with safeBlue (Invitrogen). The ACE2 band was cut out from the gel for glycan structure analysis. Briefly, the gel plugs were washed in acetonitrile, followed by subsequent steps of 20 mM ammonium bicarbonate and acetonitrile before being dried in a Speed-Vac machine. Peptide-N-glycosidase F (PNGase F) was diluted with 20 mM ammonium bicarbonate (pH 7.0) and allowed to be adsorbed directly by the gel plug. The gel plug was then covered with the same solution and allowed to incubate overnight at  $37^\circ\text{C}$ . The glycans were eluted from the gel plug by sonication in Milli-Q water three times, and the eluates were pooled, dried down, and labeled with 2AB dye (Ludger, Oxford, United Kingdom) according to the manufacturer's instructions. The glycans were cleaned up using paper chromatography and filtered using a 0.22- $\mu$ m syringe filter. Fluorescently la-

beled glycans were subsequently analyzed by high-pressure liquid chromatography (HPLC) using a normal-phase column (TSK amide 80 column). The mobile phase consisted of solvent A (50 mM ammonium formate, pH 4.4) and solvent B (acetonitrile), and the gradient used was as follows: a linear gradient from 20% to 58% solvent A at 0.4 ml/minute for 152 min followed by a linear gradient from 58% to 100% solvent A for the next 3 min. The flow rate was increased to 1.0 ml/minute and the column washed in 100% solvent A for 5 min. Following the wash step, the column was equilibrated in 20% solvent A for 22 min in preparation for the next sample run. HPLC analysis was performed using a Waters Alliance HPLC system complemented with a Waters fluorescence detector, and results were quantified using Millennium Chromatography Manager (Waters Corporation, Milford, MA). Glycan structures were identified by the calculation of glucose unit (GU) values as described previously, through comparison to known standards and sequential exoglycosidase digestion as we have done previously (35).

**Flow cytometry.** FLP-IN/ACE2 cells were cultured with complete DMEM, with or without tetracycline (1  $\mu$ g/ml) and IHVR-17028 (50  $\mu$ M), for 48 h. The cells were detached by treatment with 5 mM EDTA in PBS followed by washing once with IF buffer (1% fetal bovine serum and 0.02%  $\text{NaN}_3$  in PBS). The suspended cells were incubated with a monoclonal antibody against the myc epitope (1/250 dilution) or the fusion protein between the SARS-CoV RBD and IgG Fc for 1 h. The cells were washed three times with IF buffer and were further incubated on ice for 30 min with a secondary antibody conjugated with fluorescein isothiocyanate (FITC). After the incubation, the cells were washed three times with IF buffer and fixed with 1% formaldehyde. Flow cytometry analysis was performed by using a Beckman Coulter FC500 cytofluorometer.

**Cell fusion assays.** 293T cells seeded in 6-well plates were transfected with either pcDNA5/RFT/ACE2 or pSARS-S by using Lipofectamine 2000 (Invitrogen). At 5 h posttransfection, 293T cells were mock treated (0.2% dimethyl sulfoxide [DMSO]) or treated with 50  $\mu$ M IHVR-17028 for 48 h. The cells were then trypsinized and mixed in equal amounts between the two sets of transfected cells, with or without IHVR-17028 treatment. The mixed cells were seeded into 12-well plates at a density of  $4 \times 10^5$  cells per well. After another 24 h of incubation at 37°C, syncytium formation was inspected and imaged under a microscope.

To quantitatively measure syncytium formation, 293T cells seeded in 6-well plates were transfected with pcDNA5/RFT/ACE2 or pSARS-S and pCMV/T7 pol or pT7/Luc by using Lipofectamine 2000 (Invitrogen). At 5 h posttransfection, 293T cells were mock treated (0.2% DMSO) or treated with 50  $\mu$ M IHVR-17028 for 48 h. The cells were then trypsinized and mixed in equal amounts between the two sets of transfected cells, with or without IHVR-17028 treatment. The mixed cells were seeded into 96-well plates at a density of  $4 \times 10^4$  cells per well. After another 24 h of incubation at 37°C, cells were lysed with cell lysis buffer (Promega) for 15 min, followed by adding luciferase substrate (Promega). The firefly luciferase activities were measured by luminometry in a TopCounter instrument (PerkinElmer).

## RESULTS

### Iminosugars inhibit the transduction of lentiviral particles pseudotyped with envelope proteins from SARS-CoV and IAV.

In order to investigate the hypothesis that suppression of ER glucosidases may alter the glycan processing of viral receptors and consequently inhibit virus entry into host cells, Huh7.5 cells were treated for 3 days with a panel of four 1-deoxynojirimycin (DNJ) derivatives that have been shown previously to inhibit ER glucosidases with different potencies (13, 15, 21, 27). The cells were then infected with lentiviral particles pseudotyped with envelope proteins of seven different viruses. As shown in Fig. 1, compared to mock-treated controls, treatment with any of the four iminosugars did not apparently inhibit the transduction of lentiviral particles pseudotyped with HCV envelope proteins E1 and E2 (HCVpp), VSV G protein (VSVpp),

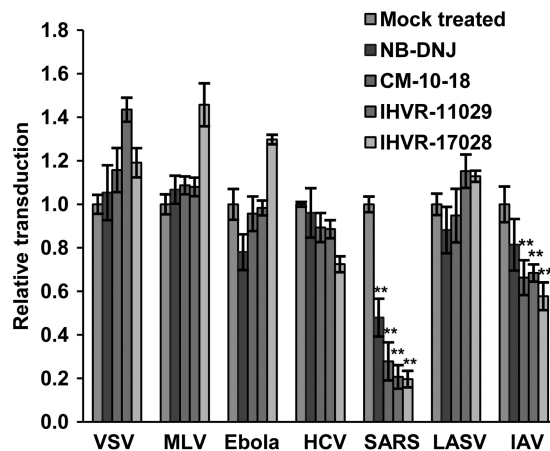


**FIG 1** Effects of iminosugars on transduction of a panel of pseudotyped lentiviral particles. Huh7.5 cells seeded in 96-well plates were mock treated (0.5% DMSO) or treated with 50  $\mu$ M iminosugar, as indicated, for 72 h, followed by inoculation of the pseudotyped lentiviral particles for 3 h. After two washes with DMEM, the cells were cultured with complete DMEM for another 72 h. Luciferase activity in the cell lysates was determined. Relative transduction efficiency represents the luciferase activity normalized to that of mock-treated cells and expressed as the mean  $\pm$  standard deviation ( $n = 6$ ). Differences in SARSpp and IAVpp transduction efficiencies between mock-treated cells and cells treated with iminosugar compounds are statistically significant (\*\*,  $P < 0.001$ ). Representative results from three independent experiments are presented.

MLV envelope protein (MLVpp), EBOV glycoprotein (EBOVpp), or LASV envelope protein (LASVpp). However, the four iminosugar compounds significantly inhibited the transduction of SARS-CoV spike glycoprotein-pseudotyped lentiviral particles (SARSpp), with a rank order of potency similar to that for the compounds to inhibit the glycan processing of HCV and bovine viral diarrhea virus (BVDV) envelope glycoproteins and the production of infectious HCV, DENV, and BVDV from infected cells (12, 13). Furthermore, except for *N*-butyl-DNJ (NB-DNJ), a weaker inhibitor of ER  $\alpha$ -glucosidases in cultured cells (12), three other, more potent iminosugars also significantly inhibited the transduction of lentiviral particles pseudotyped with IAV hemagglutinin 1 (H1) and neuraminidase 1 (N1) (IAVpp), albeit to a lesser extent. No cytotoxicity was detected for all the tested compounds by microscopic inspection under these experimental conditions. The 50% cytotoxic concentrations ( $\text{CC}_{50}$ ) of the compounds are  $>500 \mu\text{M}$  in Huh7.5 cells, as determined by MTT [3-(4,5-dimethyl-2-thiazolyl)-2,5-diphenyl-2H-tetrazolium bromide] assay (12, 27, 28). Because the only differences among the seven pseudoviral particles were in their envelope protein(s), the differential effects of iminosugars on the transduction of pseudoviral particles imply that the compounds selectively inhibited the infectious entry mediated by the envelope proteins of SARS-CoV and IAV, but not those of the other five viruses tested.

**IHVR-17028 inhibits the transduction of lentiviral particles pseudotyped with envelope proteins from SARS-CoV, HCoV-NL63, or IAV in a dose- and time-dependent manner.** SARS-CoV is a group II coronavirus and uses ACE2 as its receptor to infect host cells (24). Incidentally, HCoV-NL63, a group I human coronavirus that causes the common cold, also uses ACE2 as its receptor (25). Although the receptor binding domains of the spike proteins of the two human coronaviruses have no structural homology, they bind to distinct but overlapping sites of ACE2 to

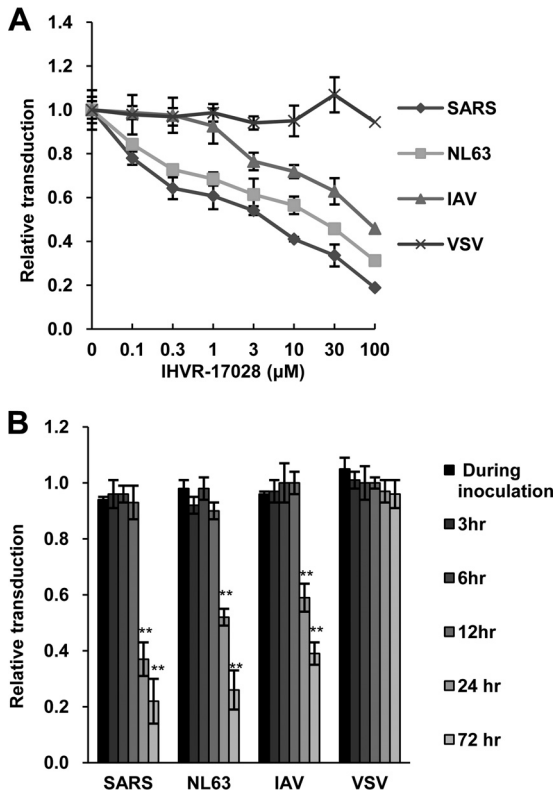


**FIG 2** IHVR-17028 inhibits pseudotyped lentiviral transduction in a dose- and time-dependent manner. (A) Huh7.5 cells were pretreated with IHVR-17028 at the indicated concentrations for 72 h, followed by infection with the indicated pseudotyped viral particles for 3 h. Luciferase activity in the cell lysates was determined at 72 h postinfection. Relative transduction efficiency represents the luciferase activity normalized to that of mock-treated cells and expressed as the mean  $\pm$  standard deviation ( $n = 6$ ). (B) Huh7.5 cells seeded in 96-well plates were pretreated with 50  $\mu$ M IHVR-17028 for the indicated periods or during infection with pseudotyped lentiviral particles for 2 h. After two washes with DMEM, the cells were cultured with complete DMEM. Luciferase activities in cell lysates were determined at 72 h postinfection. Relative transduction efficiency represents the luciferase activity normalized to that of mock-treated cells and expressed as the mean  $\pm$  standard deviation ( $n = 6$ ). Differences in SARS-CoVpp, HCoV-NL63pp, or IAVpp transduction efficiency between cells with mock and IHVR-17028 treatments for 24 h or longer are statistically significant (\*\*,  $P < 0.001$ ). Representative results from three independent experiments are presented.

initiate the infectious entry process (36). However, infection of the two viruses demonstrated differential endosomal pH and cathepsin L dependences (37, 38), suggesting that their post-receptor-binding entry events, such as endocytosis, endosomal vesicle trafficking, viral envelope glycoprotein processing, and membrane fusion, are differentially regulated. Nevertheless, if iminosugar inhibition of SARS-CoV spike protein-mediated entry is due to the alteration of ACE2 glycan structure, we anticipated that the compounds might also inhibit HCoV-NL63 spike protein-mediated entry. Indeed, the results presented in Fig. 2A showed that IHVR-17028 dose-dependently inhibited the transduction of SARSpp as well as lentiviral particles pseudotyped with the HCoV-NL63 spike protein (NL63pp). The  $EC_{50}$ s of IHVR-17028 to suppress the transduction of SARSpp, NL63pp, and IAVpp are 7.2, 22.0, and 55.3  $\mu$ M, respectively.

Because inhibition of ER glucosidases impairs only the N-

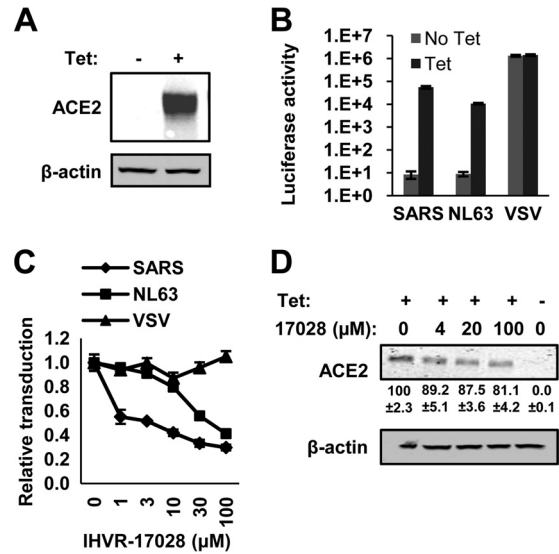


**FIG 3** IHVR-17028 dose-dependently inhibits the transduction of ACE2-expressing 293 cells by SARS-CoVpp and HCoV-NL63pp but not VSVpp. (A) An FLP-IN T Rex-derived stable cell line that inducibly (via tetracycline) expresses N-terminally myc-tagged ACE2, designated FLP-IN/ACE2, was established as described in Materials and Methods. The cells were cultured in the absence or presence of 1  $\mu$ g/ml of tetracycline for 24 h. The levels of ACE2 protein expression in cell lysates were determined by a Western blot assay with a monoclonal antibody against the myc tag.  $\beta$ -Actin served as a loading control. (B) FLP-IN/ACE2 cells were cultured in complete DMEM with or without tetracycline for 24 h, followed by infection with the indicated pseudotyped lentiviral particles. Luciferase activity was determined at 72 h postinfection. Luciferase activity is expressed as the mean  $\pm$  standard deviation ( $n = 6$ ). (C) FLP-IN/ACE2 cells were cultured in complete DMEM with tetracycline and the indicated concentrations of IHVR-17028 for 48 h and then infected with the indicated pseudotyped lentiviral particles. Luciferase activities in cell lysates were determined at 72 h postinfection. Relative transduction efficiency represents the luciferase activity normalized to that of mock-treated cells and expressed as the mean  $\pm$  standard deviation ( $n = 6$ ). (D) FLP-IN/ACE2 cells were cultured with IHVR-17028 at the indicated concentrations in the absence or presence of tetracycline for 48 h. The levels of ACE2 protein expression were determined by a Western blot assay with a monoclonal antibody against the myc tag.  $\beta$ -Actin served as a loading control. The relative amounts of ACE2 were quantified using Scion Image and expressed as percentages of the untreated control level (data are means  $\pm$  standard deviations from three independent experiments).

linked glycan metabolism of newly synthesized glycoproteins, a time-of-addition experiment was thus performed to determine the minimum times of iminosugar treatment sufficient to suppress the transduction of pseudoviral particles. As shown in Fig. 2B, it appears that the N-linked glycoproteins essential for the transduction of SARSpp, NL63pp, and IAVpp are metabolically dynamic and that a 24-h pretreatment is sufficient to disrupt pseudoviral particle transduction.

**IHVR-17028 inhibition of SARS-CoV and HCoV-NL63 spike protein-pseudotyped lentiviral transduction is ACE2 dependent.** We next focused our efforts to determine whether alteration of ACE2 glycan metabolism was responsible for iminosugar-mediated suppression of the transduction of SARSpp and NL63pp. To this end, we established a 293 cell-derived stable cell line, designated FLP-IN/ACE2, that expressed N-terminally myc-tagged human ACE2 in a Tet-inducible manner. Addition of Tet to the culture medium efficiently induced ACE2 expression (Fig. 3A) and conferred susceptibility of 293 cells to both SARSpp and

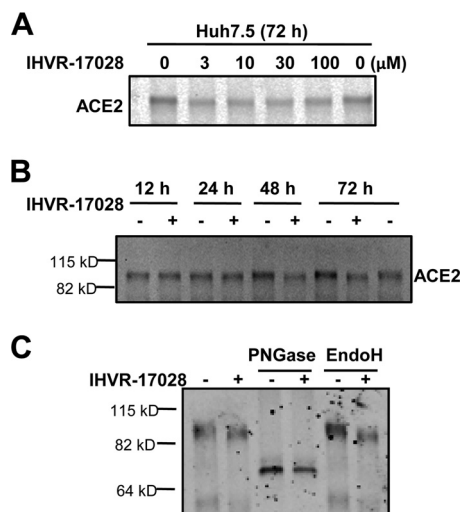


**FIG 4** IHVR-17028 treatment does not apparently change the total amount of ACE2 but alters its electrophoretic mobility. Huh7.5 cells were treated with IHVR-17028 at the indicated concentrations for 72 h (A) or treated with 50  $\mu$ M IHVR-17028 for the indicated periods (B). ACE2 in cell lysates was immunoprecipitated with an ACE2 polyclonal antibody and detected by a Western blot assay with an ACE2 polyclonal antibody. (C) 293T cells were transfected with a plasmid expressing ACE2 and treated with 50  $\mu$ M IHVR-17028 for 48 h. ACE2 in cell lysates was purified by use of protein A/G beads coated with an ACE2 polyclonal antibody. Purified ACE2 was digested by PNGase or endo H and detected by a Western blot assay. Representative results from two independent experiments are presented.

NL63pp transduction (Fig. 3B). However, as expected, expression of ACE2 did not affect the transduction of VSVpp (Fig. 3B). Consistent with the observation made with Huh7.5 cells, IHVR-17028 treatment dose-dependently inhibited SARSpp and NL63pp transduction of FLP-IN/ACE2 cells, with  $EC_{50}$ s of 2.1 and 57.2  $\mu$ M, respectively (Fig. 3C). Interestingly, Western blot analysis showed that IHVR-17028 treatment only slightly reduced the amount of total cellular ACE2 but apparently increased its migration by electrophoresis, most likely due to changes in its N-linked glycans (Fig. 3D).

#### IHVR-17028 treatment alters the glycan structure of ACE2.

In order to determine the nature of iminosugar-induced alterations of ACE2 N-linked glycans, we first confirmed with Huh7.5 cells that IHVR-17028 treatment also dose- and time-dependently induced a faster electrophoretic migration of ACE2 protein (Fig. 4A and B). Next, we showed that treatment of immunoprecipitated ACE2 protein from FLP-IN/ACE2 cells cultured in the absence or presence of IHVR-17028 with PNGase F, an amidase that cleaves between the innermost GlcNAc and asparagine residues of high-mannose, hybrid, and complex oligosaccharides from N-linked glycoproteins, resulted in ACE2 species with the same electrophoretic mobility. However, treatment with endo- $\beta$ -N-acetylglucosaminidase H (endo H), which cleaves within the chitobiose core of high-mannose and some hybrid oligosaccharides from N-linked glycoproteins, failed to remove the glycans of ACE2 (Fig. 4C). The results thus imply that the iminosugar-induced ACE2 electrophoresis mobility shift is due solely to the alteration of its N-linked glycans, not the polypeptide. Moreover, like ACE2 from mock-treated cells, the N-linked glycan of ACE2 from IHVR-17028-treated cells was also made up of complex oligosaccharides, suggesting that the N-linked glycans are still pro-

cessed to a fully complex form in cells in which ER glucosidases are inhibited.

To further characterize the structure of ACE2-linked oligosaccharides, N-linked glycan analysis was performed on the ACE2 glycoprotein following resolution of protein by one-dimensional SDS-PAGE (Fig. 5A). Briefly, each ACE2 band was excised from the gel and the N-linked glycans analyzed by normal-phase HPLC. In all cases, peak identification was made through sequential exoglycosidase digestion. Figure 5B shows the sialylated N-linked glycan profiles of ACE2 from untreated cells (top) and cells treated with 50  $\mu$ M IHVR-17028 (bottom). As the figure shows, ACE2 from untreated cells primarily contained a biantennary N-linked glycan with various levels of sialylation (A2G2 with either S1 or S2) and a core fucosylated biantennary N-linked glycan with various levels of sialylation (FcA2G2 with either S1 or S2). In addition, there were larger (tri and tetra) branched glycans with various levels of sialylation. The glycan structures were generally similar for ACE2 derived from IHVR-17028-treated cells, with several exceptions. Specifically, while the most common structures were found to be the sialylated versions of the biantennary and core fucosylated biantennary glycans, there was an overall decrease in the level of sialylation (compare S1, S2, and large branched structures between the two groups). This result explains the increased electrophoretic mobility of ACE2 proteins from iminosugar-treated cells (Fig. 4 and 5A). In addition, this result is also consistent with the endo H digestion result shown in Fig. 4C, which indicated that the ACE2 from iminosugar-treated cells contained complex glycans. In fact, it has been noted that complex glycans can be observed in the presence of the glucosidase inhibitors through the action of the Golgi endomannosidase, which can process N-linked glycan in the ER but does not allow for interaction with the host chaperones calnexin and calreticulin (39–41).

**IHVR-17028 treatment does not alter ACE2 cell surface expression and binding to SARS-CoV spike protein.** Because iminosugar treatment does not apparently reduce the amount of total cellular ACE2, it is possible that the aberrant glycan processing of ACE2 results in reduced cell surface expression and consequential inhibition of SARSpp and NL63pp transduction. However, flow cytometry analysis of intact FLP-IN/ACE2 cells cultured in the absence or presence of IHVR-17028 with an antibody against human ACE2 demonstrated that the iminosugar treatment did not affect the amount of ACE2 protein expressed on the plasma membrane (Fig. 6A and C).

The next question was whether the aberrant oligosaccharides of ACE2 from IHVR-17028-treated cells impaired the ability of the receptor molecule to bind SARS-CoV spike protein. To investigate this hypothesis, we tested the intact FLP-IN/ACE2 cells cultured in the absence or presence of IHVR-17028 for the ability to bind a fusion protein that has the receptor binding domain (RBD) of SARS spike protein fused to the N terminus of the IgG Fc fragment, which was demonstrated previously to specifically bind ACE2 and competitively inhibit SARS-CoV infection of its host cells (42). The results presented in Fig. 6B and D showed that IHVR-17028 treatment did not inhibit the fusion protein from binding ACE2-expressing cells.

**IHVR-17028 treatment reduces SARS-CoV spike protein-triggered membrane fusion.** The above-described results indicate that iminosugar suppression of SARS-CoV spike protein-mediated infectious entry is most likely not due to the inhibition of ACE2 expression on the cell surface or to impairment of its ability

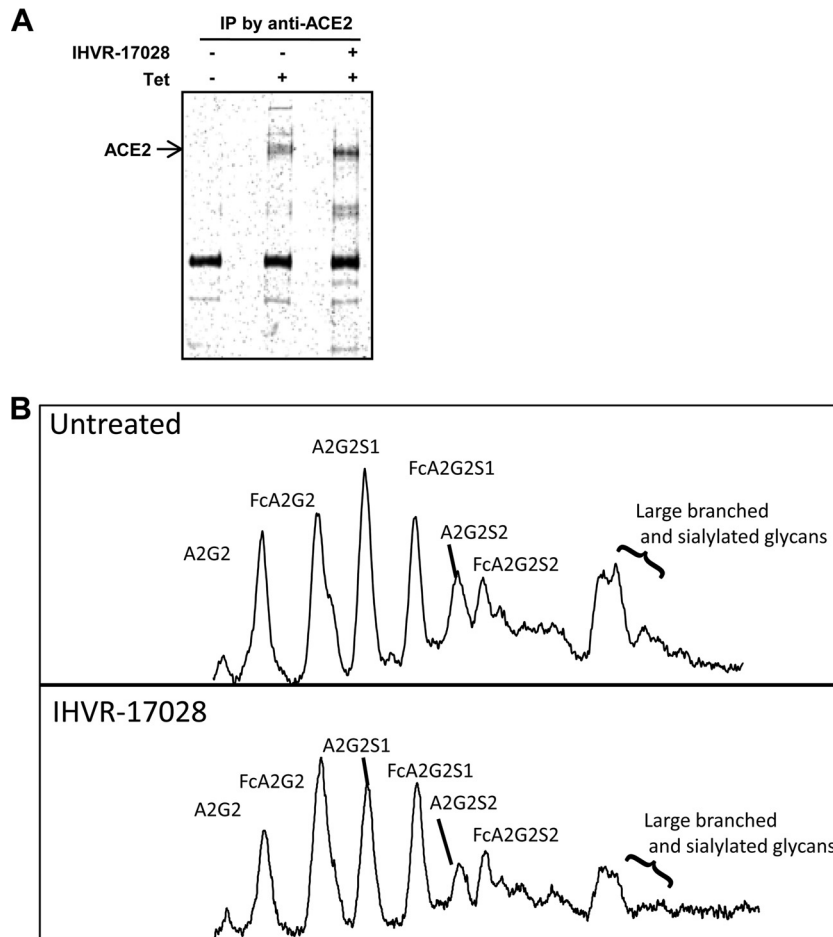


**FIG 5** IHVR-17028 treatment alters the glycan structure of ACE2. (A) FLP-IN/ACE2 cells were mock treated or treated with 50  $\mu$ M IHVR-17028 in the absence or presence of 1  $\mu$ g/ml tetracycline for 48 h and then lysed with CHAPS buffer. ACE2 protein was purified by use of protein A/G beads conjugated with polyclonal anti-ACE2 antibody and resolved by SDS-PAGE. ACE2 protein was purified by use of protein A/G beads conjugated with polyclonal anti-ACE2 antibody and resolved by SDS-PAGE. IP, immunoprecipitation. (B) The ACE2 bands were sliced from the gel and subjected to N-linked glycan analysis. The sialylated N-linked glycan profiles are shown, with the major peaks indicated. The peak labeled A2G2 is a biantennary glycan with terminal galactose residues. The peak labeled FcA2G2 is a core fucosylated biantennary glycan with terminal galactose residues. Sialylated versions of these structures are indicated as S1, containing a single sialic acid, or S2, containing two sialic acid molecules. The profiles also contain large branched glycans that contain various levels of sialylation. All peaks were identified by sequential exoglycosidase digestion. Representative results from two independent experiments are presented.

to bind the virus but to a compromise of one or multiple post-receptor-binding events. We thus investigated whether IHVR-17028 treatment of ACE2-expressing cells inhibited the membrane fusion induced by SARS-CoV spike protein binding of ACE2. Accordingly, 293T cells were transfected with a control vector, a plasmid expressing SARS-CoV spike protein, or ACE2 and cultured in the absence or presence of IHVR-17028 for 48 h. The cells were then mixed at a ratio of 1:1 with a variety of combinations and cocultured for 24 h. Membrane fusion was monitored by microscopic examination of syncytium formation. As shown in Fig. 7A, while coculture of 293T cells that expressed ACE2 and SARS-CoV spike protein in the absence of IHVR-17028 resulted in the formation of syncytia, treatment of cells that expressed either ACE2 or SARS-CoV spike protein with IHVR-17028 reduced the syncytium formation under coculture conditions.

To quantitatively measure the inhibitory effect of IHVR-17028 on membrane fusion, 293T cells were cotransfected with either plasmids encoding ACE2 and T7 polymerase or plasmids express-

ing SARS-CoV spike protein and firefly luciferase under the control of the T7 promoter (pT7/Luc). The transfected cells were mock treated or treated with IHVR-17028 for 48 h. The cells were then mixed at a 1:1 ratio and cultured for 24 h. Upon cell fusion, T7 polymerase expressed from the ACE-expressing cells will transcribe firefly luciferase mRNA from pT7/Luc received from the spike protein-expressing cells. Hence, the extent of cell fusion between the ACE2- and spike protein-expressing cells can be quantified by measuring luciferase activity in cocultured cell lysates. As expected, coculture of 293T cells expressing ACE2 and SARS-CoV spike protein without IHVR-17028 treatment induced robust luciferase expression. In agreement with previous reports that iminosugars disrupted glycan processing of SARS-CoV spike glycoprotein and inhibited the morphogenesis of the virus (43, 44), luciferase expression was completely abolished when SARS-CoV spike glycoprotein-expressing cells were treated with IHVR-17028. Interestingly, the luciferase expression was also reduced more than 60% when ACE2-expressing cells were treated with IHVR-17028 before coculture (Fig. 7B). As proof of the proper

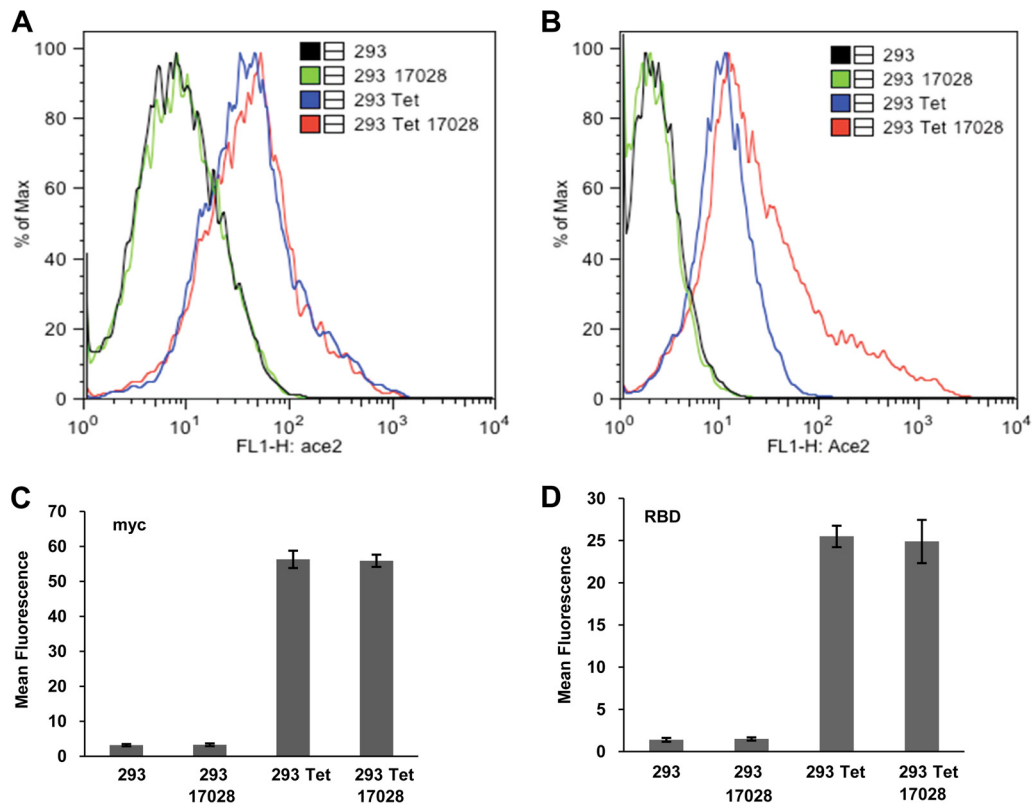


**FIG 6** IHVR-17028 treatment does not alter the cell surface expression of ACE2. FLP-IN/ACE2 cells were mock treated or treated with 50  $\mu$ M IHVR-17028 in the absence or presence of 1  $\mu$ g/ml tetracycline for 48 h. (A) Surface expression of ACE2 was examined by flow cytometry using an anti-myc antibody. (B) Binding of a SARS-CoV RBD-Ig fusion protein on the cell surface was assayed by flow cytometry. Mean fluorescence values and standard deviations from three independent experiments, obtained from cells treated under the conditions described above and stained with anti-myc antibody (C) or the SARS-CoV RBD-Ig fusion protein (D), are also presented.

effects of the iminosugar on ACE2 and SARS-CoV spike protein, IHVR-17028 treatment of the transfected 293T cells did not alter the amounts of the two proteins but enhanced the electrophoretic mobility of ACE2, while slowing the electrophoretic mobility of SARS-CoV spike protein (Fig. 7C). The latter observation is consistent with previous reports (43, 44).

## DISCUSSION

In addition to pharmacologically mobilizing host innate as well as adaptive immune responses to control viral infection, inhibition of host cellular functions required for viral replication is considered another host-targeting antiviral strategy (1). Besides the higher barrier to the emergence of drug resistance, targeting host functions commonly required by multiple viruses is an ideal approach for the development of broad-spectrum antiviral agents. In fact, extensive pharmacological studies during the last 3 decades have validated ER glucosidases as valuable host antiviral targets against many enveloped viruses (11).

Concerning the antiviral mechanism of ER glucosidase inhibitors, it is generally believed that inhibition of ER glucosidase I and/or II prevents the removal of the terminal glucose moieties on N-linked glycans and results in misfolding and retention of glycoproteins in the ER and ultimate degradation via the ER-associated degradation (ERAD) pathway (45, 46). This notion is supported by the fact that iminosugars induce the electrophoretic mobility shift of viral glycoproteins, as well as structural changes of N-

linked glycans, at lower concentrations and promote the degradation of viral glycoproteins at higher concentrations in virus-infected cells (13, 28, 44, 47). As a consequence of the abnormal trafficking and degradation of viral glycoproteins, virion assembly and secretion are inhibited (13, 48, 49). In some cases, specific viral glycoproteins with aberrant N-linked oligosaccharides can escape the ER quality control and be transported to their physiological destinations and support virion assembly and secretion. For example, human cytomegalovirus (HCMV)-infected cells continuously shed virions into the extracellular medium in the presence of CAST (50). However, due to the alterations of N-linked glycans of viral envelope proteins, infectivity of the viral particles secreted from iminosugar-treated cells is generally reduced (51–53). In fact, for most enveloped viruses investigated, reductions in both virion secretion and infectivity are responsible for the overall antiviral effects of iminosugars (52, 54, 55).

Considering host-targeting antiviral therapies, the paramount concern is the toxicity underlying the “on-target” suppression of host functions required for viral replication. Because ER glucosidases catalyze the glycan processing of both viral and host cellular glycoproteins, it is rather surprising that inhibition of ER glucosidases selectively suppresses viral replication and that iminosugars are generally well tolerated, at least for short-term therapy, in animals and humans (22, 23). A possible explanation for the selective antiviral effects of ER glucosidase inhibitors is that the viral glycoproteins are quantitatively the predominant glycoproteins made

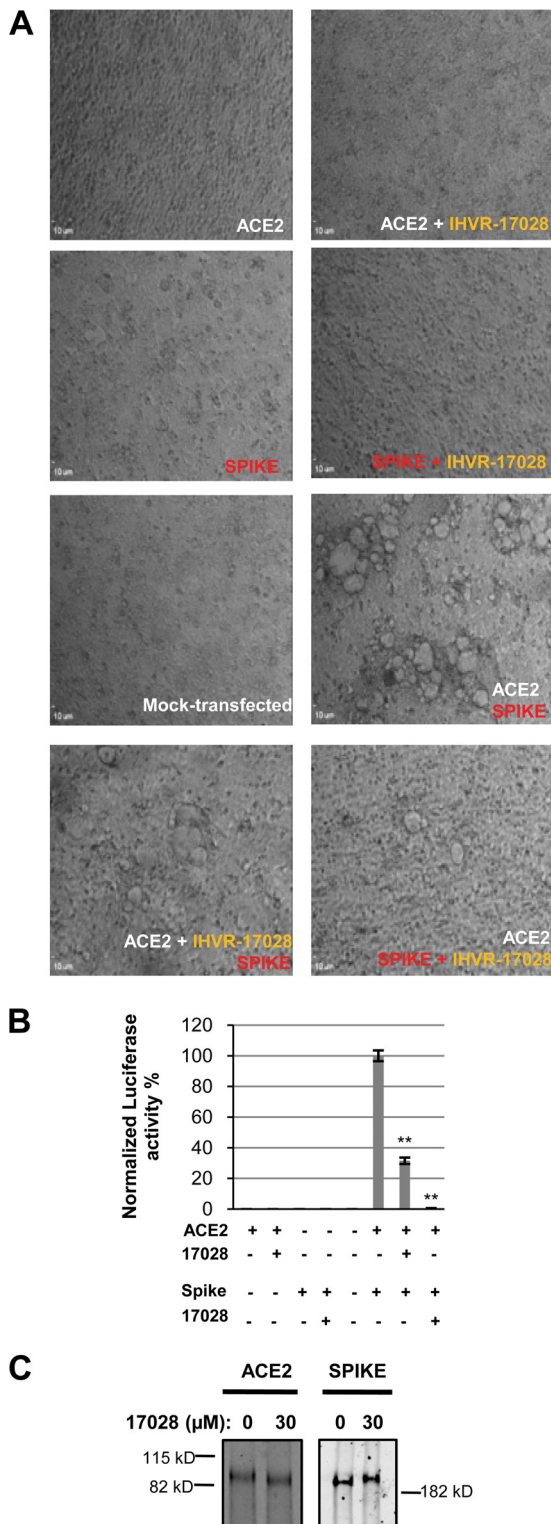


**FIG 7** Syncytium formation between SARS-CoV spike protein- and ACE2-expressing cells was inhibited by iminosugar treatment. (A) 293T cells transfected with a plasmid encoding either SARS-CoV S protein or ACE2 were mock treated or treated with 50 μM IHVR-17028 for 48 h. For syncytium formation, the cells were mixed at a 1:1 ratio and cultured for 24 h. The cultures were imaged with a Nikon microscope. (B) 293T cells cotransfected with plasmids encoding either ACE2 and T7 polymerase or SARS-CoV spike protein and T7/luciferase were mock treated or treated with 50 μM IHVR-17028 for 48 h. For syncytium formation, the cells were mixed at a 1:1 ratio and

in infected cells and are thus more vulnerable to partial inhibition of ER glucosidases. In addition, assembly of infectious virion particles relies on coordinative interaction among multiple copies of envelope glycoproteins, and misfolding of a small fraction of viral glycoprotein may lead to the failure of virion assembly.

Interestingly, a recent report on the clinical manifestation of two siblings with a rare congenital disorder of glycosylation type IIb (CDG-IIb) caused by a genetic deficiency of ER glucosidase I sheds light on the consequences of long-term suppression of ER glucosidases in humans (56). Specifically, the two siblings with CDG-IIb manifested multiple neurologic complications and severe hypogammaglobulinemia. However, the patients had no clinical evidence of an infectious diathesis, and cells derived from the patients demonstrated a reduced ability to support productive infection of multiple enveloped viruses. While the observation genetically validates the notion suggested by previous pharmacological studies that impaired N-linked glycan processing compromises host cells to support productive replication of many enveloped viruses, it also clearly indicates that long-term suppression of ER glucosidases I and/or II with more potent inhibitors may cause significant side effects, particularly in nerve and immune systems.

In this study, we investigated whether iminosugars affected the function of a specific group of host cellular glycoproteins, the viral cellular receptors. By examining the effects of iminosugars on the transduction of lentiviral particles pseudotyped with envelope proteins from eight different viruses, we demonstrated that the N-linked glycan processing of some host cellular proteins is indeed altered under the conditions where viral glycoprotein metabolism is affected. Detailed analyses of the glycan processing of ACE2 revealed that the N-linked oligosaccharides in iminosugar-treated cells can be processed through an alternative pathway that trims the N-linked glycans by cleaving the oligosaccharide chains between the internal mannose moieties by Golgi endomannosidases (39–41). The resulting N-linked glycans are further processed and matured into complex glycans in the Golgi apparatus. Moreover, alteration of N-linked glycans of ACE2 does not apparently affect its cell surface expression and binding of the SARS-CoV spike glycoprotein, but it does impair its ability to support viral envelope spike glycoprotein-triggered membrane fusion. At this moment, whether the reduced fusion activity is due to the aberrant glycan structure of ACE2 or to misfolding of the glycoprotein, a consequence of abnormal glycan processing, remains to be determined. A possible scenario is that alteration of ACE2 N-linked glycans compromises its dynamic interaction with viral envelope glycoproteins during membrane fusion and consequently inhibits SARS-CoV and CoV-NL63 glycoprotein-mediated infectious entry. Alternatively, alteration of N-linked glycans may disrupt ACE2 interaction with another cellular component(s) that facilitates the membrane fusion between virus and host cells. Nevertheless, our study does demonstrate, for the first time, that N-

cultured for 24 h. Luciferase activities in the cell lysates were determined, normalized to the mock-treated control level, and then expressed as means ± standard deviations ( $n = 4$ ). Differences in cell fusion between mock-treated and IHVR-17028-treated cells were analyzed statistically (\*\*,  $P < 0.001$ ;  $t$  test). (C) 293T cells transfected with a plasmid encoding SARS-CoV S protein or ACE2 were treated with 50 μM IHVR-17028 for 48 h and then lysed by use of CHAPS buffer. The ACE2 and SARS-CoV spike proteins were detected by Western blotting. Representative results from two independent experiments are presented.

linked glycans of ACE2 are important for virus-induced membrane fusion.

It is also interesting that IHVR-17028 treatment more potently inhibited the transduction of SARSpp than that of NL63pp in both Huh7.5 cells (Fig. 2A) and FLP-IN/ACE2 cells (Fig. 3C). This differential effect of IHVR-17028 on SARS-CoV and CoV-NL63 glycoprotein-mediated infectious entry is most likely because one or multiple post-receptor-binding events of SARS-CoV glycoprotein-mediated infectious entry are more liable to undergo the iminosugar-induced ACE2 glycan alterations.

IAV infection of cells begins with the binding of hemagglutinin (HA) to sialic acid on the cell surface. It was shown previously that sialic acid moieties on the N-linked glycans of cell plasma membrane glycoproteins are essential for IAV infection (57, 58). It can thus be speculated that inhibition of the removal of the three terminal glucose moieties from the N-linked glycans by iminosugars will disturb the further processing and addition of sialic acids to the N-linked glycans in the Golgi apparatus, which consequentially inhibits IAV infection. In agreement with our results showing that iminosugars inhibited IAV envelope protein-pseudotyped lentiviral entry (Fig. 1 and 2), the cells derived from the CDG-IIb patients also demonstrated a reduced ability to support the infectious entry of IAV (56).

In summary, our work reported herein demonstrates that suppression of ER glucosidases not only inhibits infectious virion production but also impairs the entry of selected viruses into their host cells by altering the structure and function of the N-linked glycans of their cellular receptors. The broad-spectrum antiviral activity, multiple modes of antiviral action, and great *in vivo* tolerability for short-term administrations make ER glucosidase inhibitors the ideal antiviral agents for treatment of acute viral infections, particularly viral hemorrhagic fevers and severe respiratory tract viral infections. This is because each of these medical conditions can be caused by many different viruses and is symptomatically difficult to distinguish, which makes etiologic diagnosis essential for virus-specific antiviral therapies. Moreover, both viral hemorrhagic fevers and severe respiratory tract viral infections are sometimes life-threatening and have a short time window for antiviral intervention, which also favors host-targeting broad-spectrum antiviral therapies (59–61). Fortunately, all the viruses causing these two medical conditions are enveloped viruses that are sensitive to ER glucosidase inhibitors (11).

## ACKNOWLEDGMENTS

This work was supported by NIH grant AI104636 and by The Commonwealth of Pennsylvania through the Hepatitis B Foundation.

## REFERENCES

- Lou Z, Sun Y, Rao Z. 2014. Current progress in antiviral strategies. *Trends Pharmacol Sci* 35:86–102. <http://dx.doi.org/10.1016/j.tips.2013.11.006>.
- Lin K, Galloway P. 2013. Curing a viral infection by targeting the host: the example of cyclophilin inhibitors. *Antiviral Res* 99:68–77. <http://dx.doi.org/10.1016/j.antiviral.2013.03.020>.
- de Chasse B, Meyniel-Schicklin L, Aublin-Gex A, Andre P, Lotteau V. 2012. New horizons for antiviral drug discovery from virus-host protein interaction networks. *Curr Opin Virol* 2:606–613. <http://dx.doi.org/10.1016/j.coviro.2012.09.001>.
- Meliopoulos VA, Andersen LE, Birrer KF, Simpson KJ, Lowenthal JW, Bean AG, Stamba J, Stewart CR, Tompkins SM, van Beusechem VW, Fraser I, Mhlanga M, Barichievy S, Smith Q, Leake D, Karpilow J, Buck A, Jona G, Tripp RA. 2012. Host gene targets for novel influenza therapies elucidated by high-throughput RNA interference screens. *FASEB J* 26:1372–1386. <http://dx.doi.org/10.1096/fj.11-193466>.
- Hong-Geller E, Micheva-Viteva SN. 2010. Functional gene discovery using RNA interference-based genomic screens to combat pathogen infection. *Curr Drug Discov Technol* 7:86–94. <http://dx.doi.org/10.2174/157016310793180657>.
- Watanabe T, Watanabe S, Kawaoka Y. 2010. Cellular networks involved in the influenza virus life cycle. *Cell Host Microbe* 7:427–439. <http://dx.doi.org/10.1016/j.chom.2010.05.008>.
- Furuta Y, Takahashi K, Shiraki K, Sakamoto K, Smee DF, Barnard DL, Gowen BB, Julander JG, Morrey JD. 2009. T-705 (favipiravir) and related compounds: novel broad-spectrum inhibitors of RNA viral infections. *Antiviral Res* 82:95–102. <http://dx.doi.org/10.1016/j.antiviral.2009.02.198>.
- Bray M, Raymond JL, Geisbert T, Baker RO. 2002. 3-Deazaneplanocin A induces massively increased interferon-alpha production in Ebola virus-infected mice. *Antiviral Res* 55:151–159. [http://dx.doi.org/10.1016/S0166-3542\(02\)00018-9](http://dx.doi.org/10.1016/S0166-3542(02)00018-9).
- Bray M, Driscoll J, Huggins JW. 2000. Treatment of lethal Ebola virus infection in mice with a single dose of an S-adenosyl-L-homocysteine hydrolase inhibitor. *Antiviral Res* 45:135–147. [http://dx.doi.org/10.1016/S0166-3542\(00\)00066-8](http://dx.doi.org/10.1016/S0166-3542(00)00066-8).
- Inoue K, Umehara T, Ruegg UT, Yasui F, Watanabe T, Yasuda H, Dumont JM, Scalfaro P, Yoshida M, Kohara M. 2007. Evaluation of a cyclophilin inhibitor in hepatitis C virus-infected chimeric mice *in vivo*. *Hepatology* 45:921–928. <http://dx.doi.org/10.1002/hep.21587>.
- Chang J, Block TM, Guo JT. 2013. Antiviral therapies targeting host ER alpha-glucosidases: current status and future directions. *Antiviral Res* 99:251–260. <http://dx.doi.org/10.1016/j.antiviral.2013.06.011>.
- Qu X, Pan X, Weidner J, Yu W, Alonzi D, Xu X, Butters T, Block T, Guo JT, Chang J. 2011. Inhibitors of endoplasmic reticulum alpha-glucosidases potently suppress hepatitis C virus virion assembly and release. *Antimicrob Agents Chemother* 55:1036–1044. <http://dx.doi.org/10.1128/AAC.01319-10>.
- Chang J, Wang L, Ma D, Qu X, Guo H, Xu X, Mason PM, Bourne N, Moriarty R, Gu B, Guo JT, Block TM. 2009. Novel imino sugar derivatives demonstrate potent antiviral activity against flaviviruses. *Antimicrob Agents Chemother* 53:1501–1508. <http://dx.doi.org/10.1128/AAC.01457-08>.
- Perry ST, Buck MD, Plummer EM, Penmasta RA, Batra H, Stavale EJ, Warfield KL, Dwek RA, Butters TD, Alonzi DS, Lada SM, King K, Klose B, Ramstedt U, Shresta S. 2013. An iminosugar with potent inhibition of dengue virus infection *in vivo*. *Antiviral Res* 98:35–43. <http://dx.doi.org/10.1016/j.antiviral.2013.01.004>.
- Chang J, Schul W, Butters TD, Yip A, Liu B, Goh A, Lakshminarayana SB, Alonzi D, Reinkensmeier G, Pan X, Qu X, Weidner JM, Wang L, Yu W, Borune N, Kinch MA, Rayahin JE, Moriarty R, Xu X, Shi PY, Guo JT, Block TM. 2011. Combination of alpha-glucosidase inhibitor and ribavirin for the treatment of dengue virus infection *in vitro* and *in vivo*. *Antiviral Res* 89:26–34. <http://dx.doi.org/10.1016/j.antiviral.2010.11.002>.
- Miller JL, Lachica R, Sayce AC, Williams JP, Bapat M, Dwek R, Beatty PR, Harris E, Zitzmann N. 2012. Liposome-mediated delivery of iminosugars enhances efficacy against dengue virus *in vivo*. *Antimicrob Agents Chemother* 56:6379–6386. <http://dx.doi.org/10.1128/AAC.01554-12>.
- Rathore AP, Paradkar PN, Watanabe S, Tan KH, Sung C, Connolly JE, Low J, Ooi EE, Vasudevan SG. 2011. Celgosivir treatment misfolds dengue virus NS1 protein, induces cellular pro-survival genes and protects against lethal challenge mouse model. *Antiviral Res* 92:453–460. <http://dx.doi.org/10.1016/j.antiviral.2011.10.002>.
- Watanabe S, Rathore AP, Sung C, Lu F, Khoo YM, Connolly J, Low J, Ooi EE, Lee HS, Vasudevan SG. 2012. Dose- and schedule-dependent protective efficacy of celgosivir in a lethal mouse model for dengue virus infection informs dosing regimen for a proof of concept clinical trial. *Antiviral Res* 96:32–35. <http://dx.doi.org/10.1016/j.antiviral.2012.07.008>.
- Whitby K, Pierson TC, Geiss B, Lane K, Engle M, Zhou Y, Doms RW, Diamond MS. 2005. Castanospermine, a potent inhibitor of dengue virus infection *in vitro* and *in vivo*. *J Virol* 79:8698–8706. <http://dx.doi.org/10.1128/JVI.79.14.8698-8706.2005>.
- Wu SF, Lee CJ, Liao CL, Dwek RA, Zitzmann N, Lin YL. 2002. Antiviral effects of an iminosugar derivative on flavivirus infections. *J Virol* 76:3596–3604. <http://dx.doi.org/10.1128/JVI.76.8.3596-3604.2002>.
- Chang J, Warren TK, Zhao X, Gill T, Guo F, Wang L, Comunale MA, Du

- Y, Alonzi DS, Yu W, Ye H, Liu F, Guo JT, Mehta A, Cuconati A, Butters TD, Bavari S, Xu X, Block TM. 2013. Small molecule inhibitors of ER  $\alpha$ -glucosidases are active against multiple hemorrhagic fever viruses. *Antiviral Res* 98:432–440. <http://dx.doi.org/10.1016/j.antiviral.2013.03.023>.
22. Durantel D. 2009. Celgosivir, an alpha-glucosidase I inhibitor for the potential treatment of HCV infection. *Curr Opin Invest Drugs* 10:860–870.
  23. Fischl MA, Resnick L, Coombs R, Kremer AB, Pottage JC, Jr, Fass RJ, Fife KH, Powderly WG, Collier AC, Aspinall RL. 1994. The safety and efficacy of combination N-butyl-deoxyjirimycin (SC-48334) and zidovudine in patients with HIV-1 infection and 200–500 CD4 cells/mm<sup>3</sup>. *J Acquir Immune Defic Syndr* 7:139–147.
  24. Li W, Moore MJ, Vasilieva N, Sui J, Wong SK, Berne MA, Somasundaran M, Sullivan JL, Luzuriaga K, Greenough TC, Choe H, Farzan M. 2003. Angiotensin-converting enzyme 2 is a functional receptor for the SARS coronavirus. *Nature* 426:450–454. <http://dx.doi.org/10.1038/nature02145>.
  25. Hofmann H, Pycr K, van der Hoek L, Geier M, Berkhout B, Pohlmann S. 2005. Human coronavirus NL63 employs the severe acute respiratory syndrome coronavirus receptor for cellular entry. *Proc Natl Acad Sci U S A* 102:7988–7993. <http://dx.doi.org/10.1073/pnas.0409465102>.
  26. Jiang D, Guo H, Xu C, Chang J, Gu B, Wang L, Block TM, Guo JT. 2008. Identification of three interferon-inducible cellular enzymes that inhibit the replication of hepatitis C virus. *J Virol* 82:1665–1678. <http://dx.doi.org/10.1128/JVI.02113-07>.
  27. Chang J, Warren TK, Zhao X, Gill T, Guo F, Wang L, Comunale MA, Du Y, Alonzi DS, Yu W, Ye H, Liu F, Guo JT, Mehta A, Cuconati A, Butters TD, Bavari S, Xu X, Block TM. 2013. Small molecule inhibitors of ER alpha-glucosidases are active against multiple hemorrhagic fever viruses. *Antiviral Res* 98:432–440. <http://dx.doi.org/10.1016/j.antiviral.2013.03.023>.
  28. Yu W, Gill T, Wang L, Du Y, Ye H, Qu X, Guo JT, Cuconati A, Zhao K, Block TM, Xu X, Chang J. 2012. Design, synthesis, and biological evaluation of N-alkylated deoxyjirimycin (DNJ) derivatives for the treatment of dengue virus infection. *J Med Chem* 55:6061–6075. <http://dx.doi.org/10.1021/jm300171v>.
  29. Lin HX, Feng Y, Tu X, Zhao X, Hsieh CH, Griffin L, Junop M, Zhang C. 2011. Characterization of the spike protein of human coronavirus NL63 in receptor binding and pseudotype virus entry. *Virus Res* 160:283–293. <http://dx.doi.org/10.1016/j.virusres.2011.06.029>.
  30. Zhao X, Guo F, Liu F, Cuconati A, Chang J, Block TM, Guo JT. 2014. Interferon induction of IFITM proteins promotes infection by human coronavirus OC43. *Proc Natl Acad Sci U S A* 111:6756–6761. <http://dx.doi.org/10.1073/pnas.1320856111>.
  31. He J, Choe S, Walker R, Di Marzio P, Morgan DO, Landau NR. 1995. Human immunodeficiency virus type 1 viral protein R (Vpr) arrests cells in the G<sub>2</sub> phase of the cell cycle by inhibiting p34cdc2 activity. *J Virol* 69:6705–6711.
  32. Connor RI, Chen BK, Choe S, Landau NR. 1995. Vpr is required for efficient replication of human immunodeficiency virus type-1 in mononuclear phagocytes. *Virology* 206:935–944. <http://dx.doi.org/10.1006/viro.1995.1016>.
  33. Lin HX, Feng Y, Wong G, Wang L, Li B, Zhao X, Li Y, Smail F, Zhang C. 2008. Identification of residues in the receptor-binding domain (RBD) of the spike protein of human coronavirus NL63 that are critical for the RBD-ACE2 receptor interaction. *J Gen Virol* 89:1015–1024. <http://dx.doi.org/10.1099/vir.0.83331-0>.
  34. Jiang D, Weidner JM, Qing M, Pan XB, Guo H, Xu C, Zhang X, Birk A, Chang J, Shi PY, Block TM, Guo JT. 2010. Identification of five interferon-induced cellular proteins that inhibit West Nile virus and dengue virus infections. *J Virol* 84:8332–8341. <http://dx.doi.org/10.1128/JVI.02199-09>.
  35. Guile GR, Rudd PM, Wing DR, Prime SB, Dwek RA. 1996. A rapid high-resolution high-performance liquid chromatographic method for separating glycan mixtures and analyzing oligosaccharide profiles. *Anal Biochem* 240:210–226. <http://dx.doi.org/10.1006/abio.1996.0351>.
  36. Wu K, Li W, Peng G, Li F. 2009. Crystal structure of NL63 respiratory coronavirus receptor-binding domain complexed with its human receptor. *Proc Natl Acad Sci U S A* 106:19970–19974. <http://dx.doi.org/10.1073/pnas.0908837106>.
  37. Huang IC, Bosch BJ, Li F, Farzan M, Rottier PM, Choe H. 2006. SARS-CoV, but not HCoV-NL63, utilizes cathepsins to infect cells: viral entry. *Adv Exp Med Biol* 581:335–338. [http://dx.doi.org/10.1007/978-0-387-33012-9\\_60](http://dx.doi.org/10.1007/978-0-387-33012-9_60).
  38. Huang IC, Bosch BJ, Li F, Li W, Lee KH, Ghiran S, Vasilieva N, Dermody TS, Harrison SC, Dormitzer PR, Farzan M, Rottier PJ, Choe H. 2006. SARS coronavirus, but not human coronavirus NL63, utilizes cathepsin L to infect ACE2-expressing cells. *J Biol Chem* 281:3198–3203. <http://dx.doi.org/10.1074/jbc.M508381200>.
  39. Karaivanova VK, Luan P, Spiro RG. 1998. Processing of viral envelope glycoprotein by the endomannosidase pathway: evaluation of host cell specificity. *Glycobiology* 8:725–730. <http://dx.doi.org/10.1093/glycob/8.7.725>.
  40. Rabouille CSR. 1992. Nonselective utilization of the endomannosidase pathway for processing glycoproteins by human hepatoma (HepG2) cells. *J Biol Chem* 267:11573–11578.
  41. Mehta A, Lu X, Block TM, Blumberg BS, Dwek RA. 1997. Hepatitis B virus (HBV) envelope glycoproteins vary drastically in their sensitivity to glycan processing: evidence that alteration of a single N-linked glycosylation site can regulate HBV secretion. *Proc Natl Acad Sci U S A* 94:1822–1827. <http://dx.doi.org/10.1073/pnas.94.5.1822>.
  42. Wong SK, Li W, Moore MJ, Choe H, Farzan M. 2004. A 193-amino acid fragment of the SARS coronavirus S protein efficiently binds angiotensin-converting enzyme 2. *J Biol Chem* 279:3197–3201. <http://dx.doi.org/10.1074/jbc.C300520200>.
  43. Ritchie G, Harvey DJ, Feldmann F, Stroemer U, Feldmann H, Royle L, Dwek RA, Rudd PM. 2010. Identification of N-linked carbohydrates from severe acute respiratory syndrome (SARS) spike glycoprotein. *Virology* 399:257–269. <http://dx.doi.org/10.1016/j.viro.2009.12.020>.
  44. Fukushi M, Yoshinaka Y, Matsuoka Y, Hatakeyama S, Ishizaka Y, Kirikae T, Sasazuki T, Miyoshi-Akiyama T. 2012. Monitoring of S protein maturation in the endoplasmic reticulum by calnexin is important for the infectivity of severe acute respiratory syndrome coronavirus. *J Virol* 86:11745–11753. <http://dx.doi.org/10.1128/JVI.01250-12>.
  45. Simsek E, Mehta A, Zhou T, Dwek RA, Block T. 2005. Hepatitis B virus large and middle glycoproteins are degraded by a proteasome pathway in glucosidase-inhibited cells but not in cells with functional glucosidase enzyme. *J Virol* 79:12914–12920. <http://dx.doi.org/10.1128/JVI.79.20.12914-12920.2005>.
  46. Alonzi DS, Kukushkin NV, Allman SA, Hakki Z, Williams SJ, Pierce L, Dwek RA, Butters TD. 2013. Glycoprotein misfolding in the endoplasmic reticulum: identification of released oligosaccharides reveals a second ER-associated degradation pathway for Golgi-retrieved proteins. *Cell Mol Life Sci* 70:2799–2814. <http://dx.doi.org/10.1007/s00118-013-1304-6>.
  47. Du Y, Ye H, Gill T, Wang L, Guo F, Cuconati A, Guo JT, Block TM, Chang J, Xu X. 2013. N-Alkyldeoxyjirimycin derivatives with novel terminal tertiary amide substitution for treatment of bovine viral diarrhea virus (BVDV), dengue, and Tacaribe virus infections. *Bioorg Med Chem Lett* 23:2172–2176. <http://dx.doi.org/10.1016/j.bmcl.2013.01.108>.
  48. Taylor DL, Kang MS, Brennan TM, Bridges CG, Sunkara PS, Tys AS. 1994. Inhibition of alpha-glucosidase I of the glycoprotein-processing enzymes by 6-O-butanoyl castanospermine (MDL 28,574) and its consequences in human immunodeficiency virus-infected T cells. *Antimicrob Agents Chemother* 38:1780–1787. <http://dx.doi.org/10.1128/AAC.38.8.1780>.
  49. Hammond C, Braakman I, Helenius A. 1994. Role of N-linked oligosaccharide recognition, glucose trimming, and calnexin in glycoprotein folding and quality control. *Proc Natl Acad Sci U S A* 91:913–917. <http://dx.doi.org/10.1073/pnas.91.3.913>.
  50. Taylor DL, Fellows LE, Farrar GH, Nash RJ, Taylor-Robinson D, Moberley MA, Ryder TA, Jeffries DJ, Tys AS. 1988. Loss of cytomegalovirus infectivity after treatment with castanospermine or related plant alkaloids correlates with aberrant glycoprotein synthesis. *Antiviral Res* 10:11–26. [http://dx.doi.org/10.1016/0166-3542\(88\)90011-3](http://dx.doi.org/10.1016/0166-3542(88)90011-3).
  51. Fischer PB, Collin M, Karlsson GB, James W, Butters TD, Davis SJ, Gordon S, Dwek RA, Platt FM. 1995. The alpha-glucosidase inhibitor N-butyldeoxyjirimycin inhibits human immunodeficiency virus entry at the level of post-CD4 binding. *J Virol* 69:5791–5797.
  52. Fischer PB, Karlsson GB, Dwek RA, Platt FM. 1996. N-Butyldeoxyjirimycin-mediated inhibition of human immunodeficiency virus entry correlates with impaired gp120 shedding and gp41 exposure. *J Virol* 70:7153–7160.
  53. Fischer PB, Karlsson GB, Butters TD, Dwek RA, Platt FM. 1996. N-Butyldeoxyjirimycin-mediated inhibition of human immunodeficiency virus entry correlates with changes in antibody recognition of the V1/V2 region of gp120. *J Virol* 70:7143–7152.
  54. Lazar C, Durantel D, Macovei A, Zitzmann N, Zoulim F, Dwek RA, Branza-Nichita N. 2007. Treatment of hepatitis B virus-infected cells with alpha-glucosidase inhibitors results in production of virions with altered

- molecular composition and infectivity. *Antiviral Res* 76:30–37. <http://dx.doi.org/10.1016/j.antiviral.2007.04.004>.
55. Chapel C, Garcia C, Roingard P, Zitzmann N, Dubuisson J, Dwek RA, Trepo C, Zoulim F, Durantel D. 2006. Antiviral effect of alpha-glucosidase inhibitors on viral morphogenesis and binding properties of hepatitis C virus-like particles. *J Gen Virol* 87:861–871. <http://dx.doi.org/10.1099/vir.0.81503-0>.
  56. Sadat MA, Moir S, Chun TW, Lusso P, Kaplan G, Wolfe L, Memoli MJ, He M, Vega H, Kim LJ, Huang Y, Hussein N, Nievas E, Mitchell R, Garofalo M, Louie A, Ireland DC, Grunes C, Cimbri R, Patel V, Holzapfel G, Salahuddin D, Bristol T, Adams D, Marciano BE, Hegde M, Li Y, Calvo KR, Stoddard J, Justement JS, Jacques J, Long Priel DA, Murray D, Sun P, Kuhns DB, Boerkoel CF, Chiorini JA, Di Pasquale G, Verthelyi D, Rosenzweig SD. 2014. Glycosylation, hypogammaglobulinemia, and resistance to viral infections. *N Engl J Med* 370:1615–1625. <http://dx.doi.org/10.1056/NEJMoa1302846>.
  57. Chu VC, Whittaker GR. 2004. Influenza virus entry and infection require host cell N-linked glycoprotein. *Proc Natl Acad Sci U S A* 101:18153–18158. <http://dx.doi.org/10.1073/pnas.0405172102>.
  58. Hidari KI, Yamaguchi M, Ueno F, Abe T, Yoshida K, Suzuki T. 2013. Influenza virus utilizes N-linked sialoglycans as receptors in A549 cells. *Biochem Biophys Res Commun* 436:394–399. <http://dx.doi.org/10.1016/j.bbrc.2013.05.112>.
  59. Paessler S, Walker DH. 2013. Pathogenesis of the viral hemorrhagic fevers. *Annu Rev Pathol* 8:411–440. <http://dx.doi.org/10.1146/annurev-pathol-020712-164041>.
  60. Hussell T, Godlee A, Salek-Ardakani S, Snelgrove RJ. 2012. Respiratory viral infections: knowledge based therapeutics. *Curr Opin Immunol* 24: 438–443. <http://dx.doi.org/10.1016/j.coi.2012.06.001>.
  61. Jartti T, Jartti L, Ruuskanen O, Soderlund-Venermo M. 2012. New respiratory viral infections. *Curr Opin Pulm Med* 18:271–278. <http://dx.doi.org/10.1097/MCP.0b013e328351f8d4>.